Journal of Luminescence 131 (2011) 781–785

Contents lists available at ScienceDirect

Journal of Luminescence

journal homepage: www.elsevier.com/locate/jlumin

Optical oxygen sensing materials based on a novel dirhenium(I) complex assembled in mesoporous silica

Yanhong Liu [a,b], Bin Li [a,*], Yan Cong [a,b], Liming Zhang [a], Di Fan [a], Linfang Shi [a,b]

[a] Key Laboratory of Excited State Processes, Changchun Institute of Optics, Fine Mechanics and Physics, Chinese Academy of Sciences, Changchun 130033, PR China
[b] Graduate School of the Chinese Academy of Sciences, Chinese Academy of Sciences, Beijing 100039, PR China

ARTICLE INFO

Article history:
Received 9 January 2009
Received in revised form
31 October 2010
Accepted 6 December 2010
Available online 13 December 2010

Keywords:
Oxygen sensing
Mesoporous silica
Dirhenium(I) complex

ABSTRACT

A new dirhenium(I) complex *fac*-[{Re(CO)$_3$(4,7-dinonadecyl-1,10-phenanthro -line)}$_2$ (4,4′-bipyridyl)] (trifluoromethanesulfonate)$_2$ (denoted as D-Re(I)) is assembled in MCM-41 and SBA-15 type mesoporous silica support. The emission peaks of D-Re(I) in D-Re(I)/MCM-41 and D-Re(I)/SBA-15 are observed at 522 and 517 nm, respectively. Their long excited lifetimes, which are of the order of microseconds, indicate the presence of phosphorescence emission arising from the metal to ligand charge-transfer (MLCT) transition. The luminescence intensities of D-Re(I)/MCM-41 and D-Re(I)/SBA-15 decrease remarkably with increase in the oxygen concentration, meaning that they can be used as optical oxygen sensing materials based on luminescence quenching. The ratios I_0/I_{100} of D-Re(I)/MCM-41 and D-Re(I)/SBA-15 are estimated to be 5.6 and 20.1, respectively. The obtained Stern–Volmer oxygen quenching plots of the mesoporous sensing materials could be fitted well to the two-site Demas model and Lehrer model.

1. Introduction

Determination of oxygen concentration has long been the focus in many areas ranging from atmospheric control to river pollution monitoring. In the past decade, optical oxygen sensors based on the decrease of luminescent intensity or excited-state lifetime of the sensing material as a function of oxygen concentration have become more and more attractive compared with conventional amperometric devices owing to the advantage of quick response time, no consumption of oxygen, high sensitivity and high resolution as well as continuous determination of oxygen concentrations in remote, hazardous, or in vivo environments [1–3]. In most cases, the sensing material is composed of an indicator dye dispersed within oxygen permeable support, such as polymers, sol–gel derived silica-based materials, and Langmuir–Blodgett monolayer films [4–6]. Recently, the mesoporous silica material is expected to be an effective support for the preparation of oxygen sensors with excellent performances. Owing to its three-dimensional porous structure, oxygen could diffuse within highly ordered and nearly parallel channels, which is necessary for higher sensitivity and shorter response time [7,8]. Mesoporous silica based composites represented one of the best oxygen sensing materials, employing several kinds of transition metal complexes as reported in recent years [9–14].

For the indicator dyes, or so-called probe molecules, Ru diimine [9–12] and Pt- and Pd-porphyrin [13,14] complexes mentioned above have been most widely used due to strong visible absorption, high photochemical stability, efficient luminescence, and relatively long-lived metal to ligand charge transfer (MLCT) excited states. However, the design of new high performance oxygen senor probes has always been an active research area attracting much attention, which would be an advantage for the optimization of the sensors. Properties of the transition metal complexes, including the quantum yields, τ values, and site selective binding can be systematically tailored by modifying the ligands or metal ions. In addition to these extremely popular Ru and Pt complexes, Ir(III) as well as Re(I) complexes have also attracted more and more interest [15–19] as probes in oxygen sensors. Many mononuclear rhenium(I) complexes were also investigated in the design of new luminescent probes or sensors. In 1993, Sacksteder et al. [18] reported the oxygen quenching of ReL(CO)$_3$CNR$^+$ (L=α-diimine and R=alkyl) in silicone polymer and proposed the plausible quenching mechanism that quenching is based on the collision of oxygen and the α-diimine ligand L. Because a large L would result in fewer binding sites to accommodate binding pocket, the larger the α-diimine ligand L, the higher fraction of molecules would be easily quenched. A series of ReL(CO)$_3$Cl and ReL(CO)$_3$CN complexes on copolymer supports were also investigated in oxygen sensors by Kneas et al. [19]. Among these Re(I) complexes and ReL(CO)$_3$CNR$^+$ in silicone polymer showed the highest sensitivity above forty but with relatively poor stability [18]. After that, there is almost no high performance Re(I)complex reported in oxygen sensing materials. Several kinds of new Re(I)complexes were also synthesized as analogous of Ir(III) complexes in recent years, but none of them showed high oxygen sensing performance [17]. On the other hand, photoluminescence of ligand-bridged multinuclear complexes have been widely investigated including binuclear Re(I) complexes [20]. However, to our knowledge, there have been no reports on the optical

* Corresponding author. Tel.: +86 431 86176935.
E-mail address: lib020@ciomp.ac.cn (B. Li).

0022-2313/$ - see front matter © 2010 Elsevier B.V. All rights reserved.
doi:10.1016/j.jlumin.2010.12.003

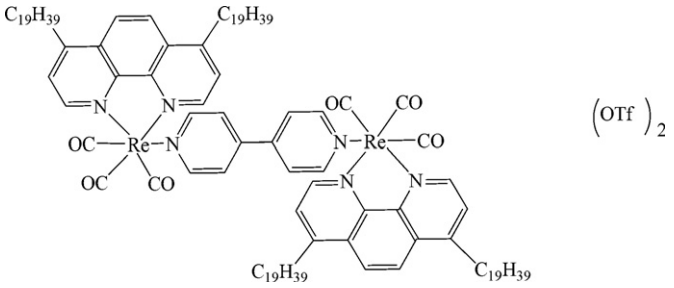

Fig. 1. Molecular structure of the D-Re(I) complex.

oxygen sensing properties of ligand-bridged multinuclear complexes. An advantage of dinuclear complexes is a higher extinction coefficient due to more luminescent centers. Additionally, dinuclear complex contains more triplet excited states, which increased the possibility of intersystem crossing and subsequently the excited state lifetime. All of the above are beneficial for oxygen sensing applications. Due to the highly ordered and nearly parallel channels, involving of Re(I) complex probes in mesoporous silica may give a chance for higher oxygen sensing performance than in polymer supports, which has not been reported yet.

In this paper, a new dirhenium(I) complex *fac*-[{$Re(CO)_3$(4,7-dinonadecyl-1,10 -phenanthroline)}$_2$ (4,4′-bipyridyl)] (trifluoromethanesulfonate)$_2$ (denoted as D-Re(I), structure shown in Fig. 1, having large α-diimine ligand *L*, were assembled in mesoporous molecular sieves MCM-41 and SBA-15 for oxygen sensor design. Oxygen sensing properties of the D-Re(I)/MCM-41 and D-Re(I)/SBA-15 composites were systematically investigated. D-Re(I)/SBA-15 exhibits high sensitivity ($I_0/I_{100}=20.1$) owing to the large α-diimine ligand d19-phen in the D-Re(I) complex.

2. Experimental section

2.1. Reagents and measurement

4,4′-dimethyl-2,2′-bipyridine (99%, Aldrich), 1-iodooctadecane (95%, Aldrich), 4,4′-bipyridine (98%, Aldrich), $Re(CO)_5Cl$ (98%, Strem), 2,2′-bipyridine (99%, Lancaster), silver trifluoromethanesulfonate (99%, Aldrich) were used as received. All other solvents for synthesis were of analytical grade and were used without further purification. ^{1}H NMR spectra were recorded on a Bruker AC 400 spectrometer. CHN elemental analysis was performed on a 240 Perkin-Elmer analyzer. Small-angle X-ray diffraction (SAXRD) patterns were recorded with a Rigaku-Dmax 2500 diffractometer using Cu Kα ($\lambda=0.15405$ nm) radiation at 0.02° (2θ) scanning step. The IR absorption spectra were measured in the region of 400–4500 cm^{-1} by a Fourier transform infrared (FTIR) spectrophotometer (Model Perkin-Elmer 580B) with a resolution of $\pm 4\ cm^{-1}$. The Re(I) ion content was analyzed by inductively coupled plasma-atomic emission spectrometry (ICP-AES) measurement with a TJA-POEMS spectrometer. The D-Re(I)/MCM-41 and D-Re(I)/SBA-15 composites were dissolved in the mixture of hydrofluoric acid and nitric acid for ICP measurement. The oxygen sensing properties based on luminescence intensity quenching of D-Re(I)/MCM-41 and D-Re(I)/SBA-15 were characterized using a Hitachi-4500 fluorescence spectrophotometer equipped with a xenon lamp (150 W) operating in the range of 200–900 nm. For the Stern–Volmer plots measurements, oxygen and nitrogen were mixed at different concentrations via gas-flow controllers and flowed directly into the gas chamber sealed with a close fitting sub-seal rubber lid equipped with two (in and out) tubes. 1 min is usually allowed between changes in the N_2/O_2 concentrations to ensure that a new equilibrium point had been established. Equilibrium was evident when the luminescence intensity remained constant ($\pm 2\%$). The sensing response curves were obtained using the same instruments. All measurements were performed at ambient temperature.

2.2. Synthesis of the D-Re(I) complex

Fig. 1 shows the molecular structure of D-Re(I). The ligand 4,7-dinonadecyl-1,10-phenanthroline (d19-phen) was obtained according to the literature [21]. The D-Re(I) was synthesized by modification of reported literatures [22–24]: 0.3 mmol $Re(CO)_5Cl$ and 0.3 mmol d19-phen were dissolved in 16 mL benzene and refluxed for 2 h under N_2 flow and *fac*-$ClRe(CO)_3$(d19-phen) was obtained by evaporating the solvent and subsequent recrystallization from dichloromethane/hexane. Then 0.2 mmol *fac*-$ClRe(CO)_3$(d19-phen) and 0.3 mmol silver trifluoromethanesulfonate (AgOTf) were mixed and refluxed in acetonitile for 8 h in the dark under N_2, from which a white residue with a clear yellow solution was obtained. After filtration, the filtrate was evaporated to give a bright yellow solid *fac*-[$(CH_3CN)Re(CO)_3$(d19-phen)]OTf (Re(I)). Finally, 0.1 mmol Re(I) and 0.05 mmol bridging ligand 4,4′-bipyridyl were refluxed in benzene for 24 h under N_2. The resulting solution was evaporated to give a bright yellow residue, which was purified by column chromatography (silica-gel using ethyl acetate/n-hexane (1:1, v/v) as the eluent). The desired dirhenium(I) complex was finally obtained. Yield: 32%. ^{1}H NMR (300 MHz, $CDCl_3$, relative to Me_4Si): δ d19-phen: 3.31 (m, 4H, $-CH_2-$), 3.19 (m, 4H, $-CH_2-$), 1.82 (m, 8H, $-CH_2-$), 1.49 (m, 8H, $-CH_2-$), 1.26 (m, 120H, $-(CH_2)_{15}-$), 0.88 (t, 12H, $J=6.6$ Hz, $-CH_3$), 9.36 (d, 4H, $J=5.5$ Hz, H at 2,9-position), 8.17 (s, 4H, H at 5,6-position), 7.88 (d, 4H, $J=5.4$ Hz, H at 3,8-position), 4,4′-bipyridyl: 8.28 (d, 4H, $J=6.7$ Hz, ortho to N), 6.68 (d, 4H, $J=6.8$ Hz, meta to N). Anal. Calcd. for $C_{118}H_{176}N_6O_{12}F_6S_2Re_2$: C, 58.54; H, 7.33; N, 3.47. Found: C, 58.80; H, 7.55; N, 3.21.

2.3. Preparation of MCM-41 and SBA-15 mesoporous silica with the physically incorporated D-Re(I) complex (denoted as D-Re(I)/MCM-41 and D-Re(I)/SBA-15)

MCM-41 and SBA-15 were synthesized according to the literatures [25,26]. The templates were removed from the mesoporous silicas by calcination at a rate of 1 °C/min and remained at 550 °C for 6 h.

The luminophor D-Re(I) complex was incorporated into mesoporous molecular sieves to obtain the assembled composite materials by the following procedure: 100 mg of the mesoporous host was added into the 10 mL dichloromethane solution of D-Re(I) complexes (1 mg), and the mixture was stirred under ambient conditions for 24 h. The resulted suspension was filtered which gave a pale yellow powder. The powder was washed repeatedly with dichloromethane until the solution was colorless under ultraviolet illumination and then dried in air. Finally, the physically encapsulated oxygen sensor materials D-Re(I)/MCM-41 and D-Re(I)/SBA-15 were obtained as pale yellow powders. Before the Stern–Volmer plots measurements, the D-Re(I)/MCM-41 and D-Re(I)/SBA-15 composites were fully grinded for about 20 min to get good enough powder that can be pressed firmly into the sample holder. This grinding process is essential for the oxygen sensing measurement to withstand the high rate gas flow.

3. Results and discussion

The SAXRD patterns of MCM-41 and D-Re(I)/MCM-41 samples, as illustrated in Fig. 2(a), both consist of a strong (1 0 0) reflection at the low angle region ranging from 1° to 2.4° (2θ) and three other reflections (1 1 0, 2 0 0, 2 1 0) located at the higher angle range, being typical of two-dimensional hexagonal structure (P6mm). The presence of these four diffraction peaks indicates that two samples have MCM-41 type

architecture with long range order [12]. Very similar SAXRD results have also been obtained in the SBA-15 systems, as shown in Fig. 2(b). The diffraction pattern in the SBA-15 systems shows three peaks which can be indexed to a hexagonal array of mesopores as for MCM-41: reflections due to the diffraction planes (1 0 0), (1 1 0), and (2 0 0) are observed. The close d_{100} spacing values of all of these samples indicate that their framework hexagonal ordering has been preserved after the incorporation of D-Re(I) into the mesoporous silica materials.

Fig. 3a shows the FTIR spectra of the D-Re(I) dichloromethane solution, D-Re(I)/MCM-41 and D-Re(I)/SBA-15. The peaks located at 2029, 1992, and 1919 cm^{-1} could be ascribed to the vibration of the three carbonyl ligands in a perturbed C_{3v} environment [32]. This is characteristic for transition metal carbonyl complexes. The three absorption peaks showed almost no shift at different environment from solution to mesoporous silica. From ICP-AES measurements, the Re content are 0.15% and 0.16% in the Re/MCM-41 and Re/SBA-15 composites, respectively.

Fig. 3b represents the photoluminescence spectra of the D-Re(I) complex in dichloromethane, the D-Re(I)/MCM-41 and D-Re(I)/SBA-15, all of which have identical band shapes. Excitation of the samples at $\lambda=400$ nm produces intense, broad and featureless emission. The emission peak of D-Re(I) in dichloromethane observed at 514 nm arises from MLCT excited state, where the emitting state is derived from a configuration involving promoting a metal d electron to a ligand π^* antibonding orbital. The emission peaks of D-Re(I)/MCM-41 and D-Re(I)/SBA-15 show red shifts of approximately 8 and 3 nm, respectively. Such red shifts are probably due to the formation of the J-aggregates, which would lead to bathochromic shift in transition energy after assembly within the mesoporous silica support [32].

Fig. 4 shows the room temperature spectral response of D-Re(I)/MCM-41 and D-Re(I)/SBA-15 under different oxygen concentrations. It is found that the relative emission intensity decreases markedly as the oxygen volume fraction increased and the emission peak does not shift or change in shape. The luminescent intensities of D-Re(I)/MCM-41 and D-Re(I)/SBA-15 decreased by 82.6% and 95.2%, respectively, upon changing from pure nitrogen to pure oxygen conditions, which are promising as sensing probes due to very high degrees of quenching.

Performance of optical sensors based on the luminescence quenching is examined by the Stern–Volmer equation. For well behaved oxygen sensing materials in which the luminophor was dispersed uniformly within homogeneous media, the intensity I and lifetime τ of the luminophor fit the linear Stern–Volmer equation [27]

$$I_0/I = \tau_0/\tau = 1 + K_{SV} pO_2 = 1 + K_q \tau_0 pO_2 \quad (1)$$

where pO_2 is the partial pressure of oxygen at 1 atmosphere pressure, τ_0 and τ are lifetimes, I_0 and I are intensities. The subscript 0 denotes the value in the absence of quencher. K_{SV} is the Stern–Volmer constant. K_q is the bimolecular quenching constant. A plot of I_0/I or τ_0/τ versus oxygen concentration should give a linear relationship with a slope of K_{SV}, and an intercept of 1 on the y-axis. The lifetime decay of luminophore in homogeneous media can be described by a single exponential equation [28]

$$I(t) = \alpha \exp(-t/\tau) \quad (2)$$

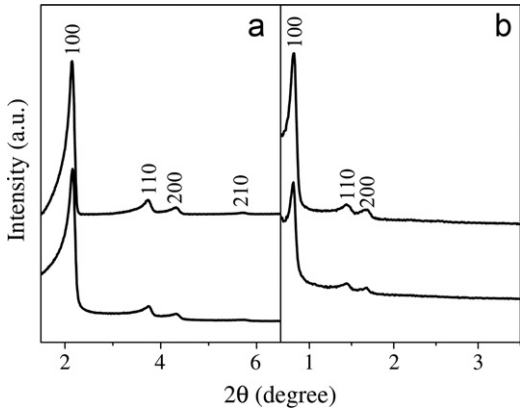

Fig. 2. (a) SAXRD patterns of MCM-41 (top) and D-Re(I) /MCM-41 (bottom). (b) SAXRD patterns of SBA-15 (top) and D-Re(I) /SBA-15 (bottom).

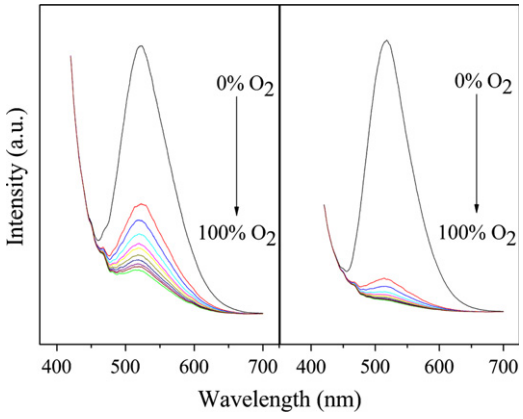

Fig. 4. Emission spectra of the D-Re(I)/MCM-41 (left) and D-Re(I)/SBA-15 (right) measured at different oxygen volume fractions ($\lambda_{ex}=400$ nm).

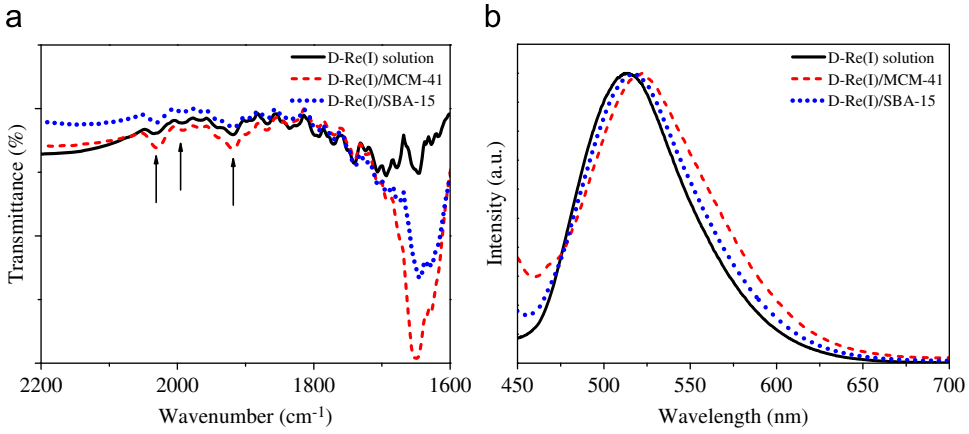

Fig. 3. (a) FTIR spectra of the D-Re(I)/MCM-41 (dash lines), D-Re(I)/SBA-15 (dot lines) and the complex D-Re(I) in anhydrous dichlormethane (solid lines). (b) Emission spectra of the D-Re(I)/MCM-41 (dash lines), D-Re(I)/SBA-15 (dot lines) and the complex D-Re(I) in anhydrous dichlormethane (solid lines) with $\lambda_{ex}=400$ nm.

where $I(t)$ is the luminescence intensity at time t, and α is the pre-exponential factor.

Fig. 5 presents the intensity-based Stern–Volmer plots for D-Re(I)/MCM-41 and D-Re(I)/SBA-15. As shown in Fig. 5, the Stern–Volmer oxygen quenching plots of D-Re(I)/MCM-41 and D-Re(I)/SBA-15 appear to deviate from linearity especially at low O_2 concentration. The downward curvature plots necessitate a more complex model than a single species quenched bimolecularly.

When quenching takes place in a solid support, the nonlinear Stern–Volmer equation is often the case, in which Demas two-site model could have excellent ability to fit the experiment data. In this model, the straight-line intensity Stern–Volmer equation [28] then becomes

$$\frac{I_0}{I} = \frac{1}{f_{01}/(1+K_{SV1}pO_2)+(1-f_{01})/(1+K_{SV2}pO_2)} \tag{3}$$

where f_{01} and $(1-f_{01})$ values are the fraction of each of the two sites contributing to the unquenched intensity, and K_{SVi} values are the associated Stern–Volmer quenching constants for the two sites, one of which is easy to be quenched but the other is not. At low oxygen concentration, easily accessible luminescence molecules are quenched more effectively, whereas the quenching responses at high oxygen concentrations are increasingly dominated by the less accessible domains. Meanwhile, when $K_{SV2}=0$, the Demas model collapses to the Lehrer model [29,30], which is also able to fit the experiment data reasonably. The equation is shown below.

$$\frac{I_0}{I} = \frac{1}{f_{01}/(1+K_{SV1}pO_2)+(1-f_{01})} \tag{4}$$

It is worth noting that either Demas two-site model or Lehrer model can be used to fit the intensity-quenching curves of all of these samples. Table 1 lists the intensity-based Stern–Volmer oxygen quenching fitting parameters: the quenching constants, K_{SV1}, K_{SV2} and the fractional contributions of the two-site components. It can be seen that Demas two-site model is more effective at fitting intensity data. The origin of the nonlinearity is a result of the luminophor molecules existing in two sites within the mesoporous silica materials in which one site is more heavily quenched than the other.

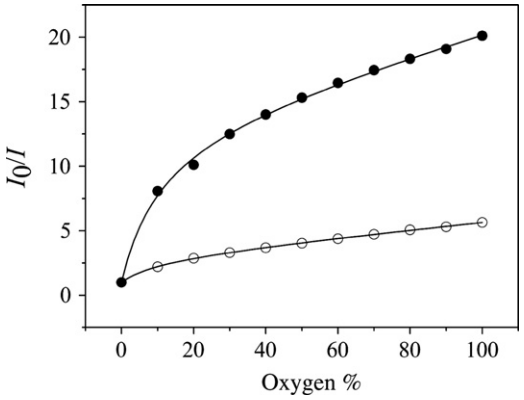

Fig. 5. Stern–Volmer plots of D-Re(I)/MCM-41 (the empty one) and D-Re(I) /SBA-15 (the solid one). The solid lines represent the best fit using the Demas two-site model.

In these Lehrer and Demas two-site models mentioned above, there are two excited-state lifetime components for the luminescence species, and the excited lifetime decay analysis may be described by [13]

$$I(t) = \alpha_1 \exp(-t/\tau_1)+\alpha_2 \exp(-t/\tau_2) \tag{5}$$

where $I(t)$ represents the fluorescence intensity at time t, the subscripts 1 and 2 denote the assigned lifetime components, and α_i denotes the pre-exponential factors. The intensity-weighted mean lifetime τ_m can be calculated with the expression: [28]

$$\langle \tau_m \rangle = \sum_{i=1}^{2} \alpha_i \tau_i \Big/ \sum_{i=1}^{2} \alpha_i \tag{6}$$

The unquenched lifetimes of the different mesoporous oxygen sensing materials under N_2 atmosphere are measured as shown in Table 2. Both of the data are found to be well-fit by the double exponential Eq. (6), which further confirms that the Re(I) ions occupy the microscopic scale heterogeneous local environment in the mesoporous silica materials MCM-41 and SBA-15. The result of the excited-state intensity decay profile is consistent with the Stern–Volmer plot.

The oxygen-quenching sensitivities I_0/I_{100} (I_{100} is the luminescent intensity under 100% oxygen) of D-Re(I)/MCM-41 and D-Re(I)/SBA-15 are estimated to be 5.6 and 20.1, respectively. It is well known that a sensor with I_0/I_{100} more than 3.0 is a suitable oxygen sensing device, so D-Re(I)/MCM-41 and D-Re(I)/SBA-15 could be used to develop oxygen sensing materials. The high sensitivity may be ascribed to the large α-diimine ligand d19-phen in the D-Re(I) complex. In previous work, Sacksteder et al. [18] reported the plausible quenching mechanism, that quenching is based on the collision of oxygen and the α-diimine ligand L. Because a large L would result in fewer binding sites to accommodate binding pocket, the larger the α-diimine ligand L, the larger fraction of molecules would be easily quenched. Additionally, D-Re(I)/SBA-15 demonstrated higher sensitivity in comparison to D-Re(I)/MCM-41. This phenomenon can be explained as following, though the detailed mechanism is still unclear. According to Eq. (1), the main differences in the sensitivity are the unquenched photoluminescence mean lifetime $\langle \tau_0 \rangle$ (as shown in Table 2) and the bimolecular quenching constant K_q. Because of the nonexponential decay of the samples, the mean lifetime $\langle \tau_0 \rangle$ was considered here. The lifetimes of the dye in solution, MCM-41 and SBA-15 are 4.53, 3.94 and 8.00 μs, respectively. It is well known that the movement of the probe molecules in solution is relatively free. However, when the molecules are dispersed in the pores of SBA-15, the rigid inorganic walls largely restrict their vibration, resulting in the decrease of the non-radiative transitions caused by vibration; hence, the increase of the lifetime. The shorter lifetime of D-Re(I)/MCM-41 may be due to the –OH quenching effect,

Table 2
Decay constants of excited-state lifetime curves of D-Re(I)/MCM-41 and D-Re(I)/SBA-15.

Sample	Gas	α_1	τ_1 (μs)	α_2	τ_2 (μs)	$\langle \tau_0 \rangle$ (μs)	r^2
D-Re(I)/MCM-41	N_2	0.16	2.45	0.06	7.93	3.94	0.9990
D-Re(I)/SBA-15	N_2	0.10	4.26	0.09	12.16	8.00	0.9989

Table 1
Intensity-based Stern–Volmer oxygen quenching parameters of the samples from the fitting employing different models, Lehrer model and Demas two-site model.

	Demas two-site model				Lehrer model		
	K_{SV1} ($O_2\%^{-1}$)	K_{SV2} ($O_2\%^{-1}$)	f_{01}	r^2	K_{SV1} ($O_2\%^{-1}$)	f_{01}	r^2
D-Re(I)/MCM-41	0.2801	0.0089	0.7117	0.9998	0.1239	0.8830	0.9913
D-Re(I)/SBA-15	1.2872	0.0054	0.9345	0.9985	0.7771	0.9606	0.9909

which plays an important role in the silica based oxygen sensing materials [12,33]. Compared with D-Re(I)/SBA-15, the smaller pore in MCM-41 gives a shorter distance between the −OH group and the probe molecules and thus a higher quenching probability. To test whether lifetime $\langle\tau_0\rangle$ can be the only scaling parameter, $[(I_0/I)-1]/\langle\tau_0\rangle$ is plotted against oxygen concentration [31], as shown in Fig. 6. It can be seen that this renormalization of the data brings the plots closer together, but the difference still exists. Meanwhile, it is well known that the pore diameter of SBA-15 is larger than MCM-41. And the enhanced sensitivity may be partly due to a more rapid diffusion of oxygen in SBA-15 than that in MCM-41.

Besides sensitivity, short response time is also important for oxygen sensors. Fig. 7 shows the typical dynamic response of the samples on exposure to pure N_2 and O_2 atmosphere varied periodically. From this time dependent measurement, the 95% response time ($t\downarrow$) and 95% recovery time ($t\uparrow$) in an alternating atmosphere of pure N_2 and O_2 can be calculated. Generally, the values are defined as the time taken for a sample to attain 95% of its total emission intensity change when the gas is changed from pure N_2 to pure O_2 ($t\downarrow$) and from pure O_2 to pure N_2 ($t\uparrow$), respectively. The $t\downarrow$ values of D-Re(I)/MCM-41 and D-Re(I)/SBA-15 are about 19 and 7 s and the $t\uparrow$ values are estimated to be 41 and 43 s, respectively. This result shows that the response time is shorter than the recovery time distinctly and this obvious difference can be explained by the stronger adsorption of oxygen than that of nitrogen on the silica surface [13]. It is well known that the reproducibility of oxygen sensing materials under irradiation is one of the key analytical characters of merit for practical applications, which allows monitoring of an increasing and decreasing pO_2 continuously. As shown in Fig. 7, stable and reproducible signals upon repeated exposure to oxygen/nitrogen cycles were also obtained for both of the D-Re(I)/MCM-41 and D-Re(I)/SBA-15.

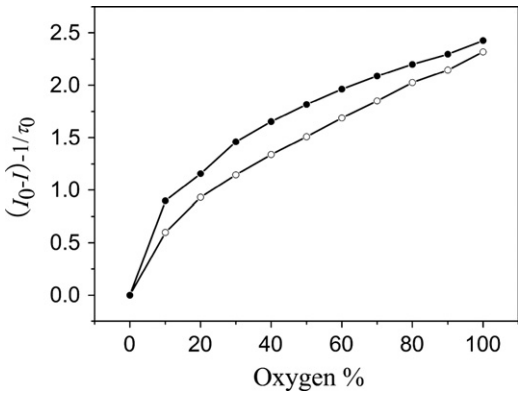

Fig. 6. Intensity-based Stern–Volmer plots scaled by the reciprocal unquenched mean lifetime $\langle\tau_0\rangle$ for D-Re(I)/MCM-41 (the empty one) and D-Re(I)/SBA-15 (the solid one).

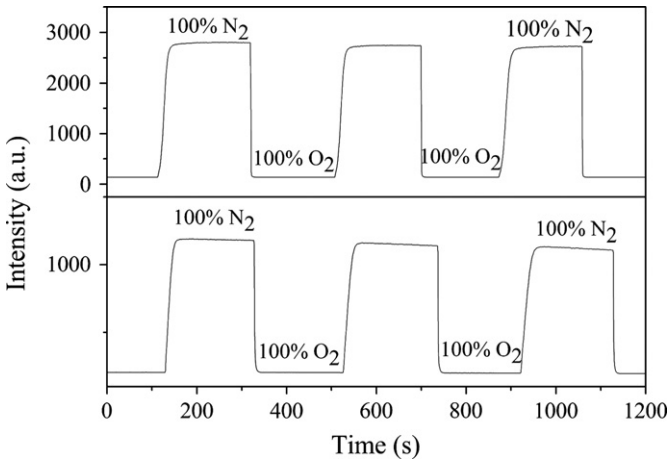

Fig. 7. Quenching responses and relative emission changes vs. time of D-Re(I)/MCM-41 (bottom) and D-Re(I)/SBA-15 (top) oxygen sensing materials on periodically cycling from 100% nitrogen to 100% oxygen atmosphere.

4. Conclusion

In this work, a new dirhenium(I) complex D-Re(I) was synthesized and assembled in mesoporous silica materials MCM-41 and SBA-15, which were investigated in view of the application in optical oxygen sensors. The quenching sensitivities of D-Re(I)/MCM-41 and D-Re(I)/SBA-15 are estimated to be 5.6 and 20.1, respectively. The high sensitivity may be ascribed to the large α-diimine ligand d19-phen in the D-Re(I) complex. Additionally, stable and reproducible signals were obtained upon repeated exposure to oxygen/nitrogen cycles for both of the D-Re(I)/MCM-41 and D-Re(I)/SBA-15. The signal reproducibility plus relatively high sensitivity make D-Re(I)/SBA-15 a promising potential oxygen sensor.

Acknowledgments

The authors gratefully thank the financial supports from the National Natural Science Foundations of China (Grant No. 50872130) and the Science and Technology Developing Project of Jilin Province (Grant No. 20100533).

References

[1] O.S. Wolfbeis, Anal. Chem. 80 (2008) 4269.
[2] J.N. Demas, B.A. DeGraff, Coord. Chem. Rev. 211 (2001) 317.
[3] Y. Amao, Microchim. Acta. 143 (2003) 1.
[4] Z. Wang, A.R. McWilliams, C.E.B. Evans, X. Lu, S. Chung, M.A. Winnik, I. Manners, Adv. Funct. Mater. 12 (2002) 415.
[5] S. Anastasova, M. Milanova, E. Kashchieva, H. Funakubo, T. Kamo, N. Grozev, P. Stefanov, D. Todorovsky, Appl. Surf. Sci. 254 (2008) 1545.
[6] B.W.K. Chu, V.W.W. Yam, Langmiur 22 (2006) 7437.
[7] C. Huo, H. Zhang, B. Yang, P. Zhang, Y. Wang, Inorg. Chem. 45 (2006) 4735.
[8] H.D. Zhang, Y.H. Sun, K.Q. Ye, P Zhang, Y Wang, J. Mater. Chem. 15 (2005) 3181.
[9] P. Payra, P.K. Dutta, Microporous Mesoporous Mater. 64 (2003) 109.
[10] E.R. Carraway, J.N. Demas, B.A. DeGraff, J.R. Bacon, Anal. Chem. 63 (1991) 337.
[11] B.H. Han, I. Manners, M.A. Winnik, Chem. Mater. 17 (2005) 3160.
[12] B. Lei, B. Li, H. Zhang, S. Lu, Z. Zheng, W. Li, Y. Wang., Adv. Funct. Mater. 16 (2006) 1883.
[13] P. Douglas, K. Eaton, Sens. Actuators B 82 (2002) 200.
[14] S. Cheng, C. Lee, C. Yang, F. Tseng, C. Moud, L. Lo, J. Mater. Chem. 19 (2009) 1252.
[15] A.L. Medina-Castillo, J.F. Fernández-Sánchez, C. Klein, M.K. Nazeeruddin, A. Segura-Carretero, A. Fernández-Gutiérrez, M. Graetzelc, U.E. Spichiger-Kellerb, Analyst 132 (2007) 929.
[16] J.F. Ferńandez-Sanchez, T. Roth, R. Cannas, M.K. Nazeeruddin, S. Spichiger, M. Graetzel, U.E. Spichiger-Keller, Talanta 71 (2007) 242.
[17] H. Loan, W. Zhuo, Y. Jian, S. Valentina, L. Alan, M. Ian, A.W. Mitchell, Chem. Mater. 17 (2005) 4765.
[18] L.A. Sacksteder, J.N. Demas, B.A. DeGraff, Anal. Chem. 5 (1993) 3480.
[19] K.A. Kneas, W.Y. Xu, J.N. Demas, B.A. DeGraff, A.P. Zipp, J. Fluo. 8 (1998) 295.
[20] S. Vaduvescu, P.G. Potvin, Euro. J. Inorg. Chem. 8 (2004) 1763.
[21] A.R. Katritzky, Q.H. Long, N. Malhotra, Synthesis (1992) 911.
[22] C. Kutal, A.J. Corbin, G. Ferraudi, O. Geiger, Organometallics 4 (1985) 2161.
[23] V.W.W. Yam, K.M.C. Wong, K.K. Cheung, Organometallics 16 (1997) 1729.
[24] A.R. de Leon, Girlie N. Sison, S.J. Borg, Innovations Chem. Biol. 17 (2008) 175.
[25] B. Onida, B. Bonelli, L. Flora, G. Geobaldo, C.O. Arean, E. Garrone, Chem. Comm. (2001) 2216.
[26] D. Zhao, Q. Huo, J. Feng, B.F. Chmelka, G.D. Stucky, J. Am. Chem. Soc. 120 (1998) 6024.
[27] V.O. Stern, M. Volmer, Physik. Zeitschr 20 (1919) 183.
[28] B.H. Han, I. Manners, M.A. Winnik, Anal. Chem. 77 (2005) 8075.
[29] Y. Tang, E.C. Tehan, Z. Tao, F.V. Bright, Anal. Chem. 75 (2003) 2407.
[30] S.S. Lehrer, Biochemistry 10 (1970) 3254.
[31] A.A. Marti, G. Mezei, L. Maldonado, G. Paralitici, R.G. Raptis, J.L. Colon, Eur. J. Inorg. Chem. 2005 (2005) 118.
[32] E. Gianotti, C.A. Bertolino, C. Benzi, et al., ACS Appl. Mater. Inter. 1 (2009) 678.
[33] Q.H. Xu, L.S. Li, X.S. Liu, R.R. Xu, Chem. Mater. 14 (2002) 549.